

NeoPalAna: Neoadjuvant Palbociclib, a Cyclin-Dependent Kinase 4/6 Inhibitor, and Anastrozole for Clinical Stage 2 or 3 Estrogen Receptor-Positive Breast Cancer



Cynthia X. Ma¹, Feng Gao², Jingqin Luo², Donald W. Northfelt³, Matthew Goetz⁴, Andres Forero⁵, Jeremy Hoog¹, Michael Naughton¹, Foluso Ademuyiwa¹, Rama Suresh¹, Karen S. Anderson⁵, Julie Margenthaler⁶, Rebecca Aft⁶, Timothy Hobday⁴, Timothy Moynihan⁴, William Gillanders⁶, Amy Cyr⁶, Timothy J. Eberlein⁶, Tina Hieken⁷, Helen Krontiras⁸, Zhanfang Guo¹, Michelle V. Lee⁹, Nicholas C. Spies¹⁰, Zachary L. Skidmore¹⁰, Obi L. Griffith^{10,11}, Malachi Griffith^{10,11}, Shana Thomas¹, Caroline Bumb¹, Kiran Vij¹, Cynthia Huang Bartlett¹², Maria Koehler¹², Hussam Al-Kateb¹³, Souzan Sanati¹³, and Matthew J. Ellis¹⁴

Abstract

Purpose: Cyclin-dependent kinase (CDK) 4/6 drives cell proliferation in estrogen receptor-positive (ER⁺) breast cancer. This single-arm phase II neoadjuvant trial (NeoPalAna) assessed the antiproliferative activity of the CDK4/6 inhibitor palbociclib in primary breast cancer as a prelude to adjuvant studies.

Experimental Design: Eligible patients with clinical stage II/III ER⁺/HER2⁻ breast cancer received anastrozole 1 mg daily for 4 weeks (cycle 0; with goserelin if premenopausal), followed by adding palbociclib (125 mg daily on days 1–21) on cycle 1 day 1 (C1D1) for four 28-day cycles unless C1D15 Ki67 > 10%, in which case patients went off study due to inadequate response. Anastrozole was continued until surgery, which occurred 3 to 5 weeks after palbociclib exposure. Later patients received additional 10 to 12 days of palbociclib (Cycle 5) immediately before surgery. Serial biopsies at baseline, C1D1, C1D15, and surgery were

analyzed for Ki67, gene expression, and mutation profiles. The primary endpoint was complete cell cycle arrest (CCCA: central Ki67 ≤ 2.7%).

Results: Fifty patients enrolled. The CCCA rate was significantly higher after adding palbociclib to anastrozole (C1D15 87% vs. C1D1 26%, *P* < 0.001). Palbociclib enhanced cell-cycle control over anastrozole monotherapy regardless of luminal subtype (A vs. B) and *PIK3CA* status with activity observed across a broad range of clinicopathologic and mutation profiles. Ki67 recovery at surgery following palbociclib washout was suppressed by cycle 5 palbociclib. Resistance was associated with nonluminal subtypes and persistent E2F-target gene expression.

Conclusions: Palbociclib is an active antiproliferative agent for early-stage breast cancer resistant to anastrozole; however, prolonged administration may be necessary to maintain its effect. *Clin Cancer Res*; 23(15); 4055–65. ©2017 AACR.

Introduction

The cyclin-dependent kinase (CDK) 4/6 in association with D-type cyclins promotes G₁-S phase transition through phosphor-

ylation of the retinoblastoma susceptibility (*RB1*) gene product (Rb) and other members of the pocket protein family (p107 and p130; refs. 1–4). Hyperphosphorylated Rb releases E2F and

¹Division of Oncology, Department of Internal Medicine, Washington University School of Medicine, St. Louis, Missouri. ²Division of Public Health Science, Siteman Cancer Center Biostatistics Core, Washington University School of Medicine, St. Louis, Missouri. ³Division of Hematology and Medical Oncology, Mayo Clinic, Phoenix, Arizona. ⁴Department of Medical Oncology, Mayo Clinic, Rochester, Minnesota. ⁵Department of Hematology and Oncology, University of Alabama at Birmingham, Birmingham, Alabama. ⁶Section of Endocrine and Oncologic Surgery, Department of Surgery, Washington University School of Medicine, St. Louis, Missouri. ⁷Department of Surgery, Mayo Clinic, Rochester, Minnesota. ⁸Department of Surgery, University of Alabama at Birmingham, Birmingham, Alabama. ⁹Department of Radiology, Washington University School of Medicine, St. Louis, Missouri. ¹⁰McDonnell Genome Institute, Washington University School of Medicine, St. Louis, Missouri. ¹¹Department of Genetics, Washington University School of Medicine, St. Louis, Missouri. ¹²Pfizer Pharmaceuticals, New York, New York. ¹³Department of Pathology and Immunology, Washington University School of Medicine, St. Louis, Missouri. ¹⁴Lester and Sue Smith Breast Center, Baylor College of Medicine, Houston, Texas.

Note: Supplementary data for this article are available at Clinical Cancer Research Online (<http://clincancerres.aacrjournals.org/>).

Prior Presentation: Presented in part at the 2015 Annual San Antonio Breast Cancer Symposium.

Corresponding Authors: Cynthia X. Ma, Washington University School of Medicine, 3rd Floor 4515 McKinley Research Building, Campus Box 8076, St. Louis, MO 63110. Phone: 314-362-9383; Fax: 314-747-9320; E-mail: cynthiamx@wustl.edu; and Matthew J. Ellis, Director of the Lester and Sue Smith Breast Center, Baylor College of Medicine, One Baylor Plaza, 320A Cullen, MS 600, Houston TX 77030. Phone: 713-798-1640; E-mail: mjellis@bcm.edu

doi: 10.1158/1078-0432.CCR-16-3206

©2017 American Association for Cancer Research.

Translational Relevance

Cyclin-dependent kinase (CDK) 4/6 plays an important role in driving cell-cycle progression in estrogen receptor–positive (ER⁺) breast cancer. The NeoPalAna trial therefore evaluated a CDK4/6 inhibitor in the neoadjuvant setting. Anastrozole monotherapy followed by the addition of palbociclib allowed an individual assessment of the degree to which CDK4/6 inhibition added to aromatase inhibitor (AI) treatment. Additional proliferation suppression by palbociclib over anastrozole alone was observed across a wide range of clinicopathologic and mutation backgrounds, including those with marked resistance to AI treatment. However, palbociclib antiproliferative effects were rapidly lost after CDK4/6 treatment was held for surgery, thus justifying prolonged therapy in the adjuvant setting. The observation of palbociclib resistance in the two nonluminal ER⁺ breast cancers, including one with an *RB1* deletion, indicates the importance of molecular subtype and *RB1* status determination in patient selection.

DP transcription factors, which activate the expression of genes required for cell proliferation (5). As cyclin D1 is a direct transcriptional target of estrogen receptor (ER), there is a direct association between ER signaling and CDK4/6 activation (6–9). In addition, estrogen-independent CDK4/6 activation occurs as a result of other mitogenic signaling or genomic alterations, leading to endocrine resistance (10).

Palbociclib is a potent selective inhibitor of CDK4/6 (11) which exerts synergistic antitumor effect when combined with endocrine therapy in both endocrine-sensitive and -resistant luminal breast cancers (12). The addition of palbociclib to endocrine therapy significantly improved progression-free survival (PFS) in patients with hormone receptor–positive, HER2-negative metastatic breast cancer (13–16). The effect of palbociclib in combination with endocrine therapy in early stage disease had not been determined. We therefore conducted a neoadjuvant phase II trial (NeoPalAna, ClinicalTrials.gov#: NCT01723774) to determine the antiproliferative activity of palbociclib when added to anastrozole in patients with newly diagnosed clinical stage II/III ER⁺/HER2⁻ breast cancer as a prelude to adjuvant studies and to discover predictive biomarkers potentially useful for defining the appropriate adjuvant population.

The primary objective was to determine whether the addition of anastrozole to palbociclib induces a higher rate of complete cell cycle arrest (CCCA: Ki67 ≤ 2.7%) than that achieved by anastrozole alone administered as initial therapy. The primary endpoint was chosen based on the long-term follow-up data of several neoadjuvant endocrine therapy trials which demonstrated that the 2.7% Ki67 cut-point (natural log of one) during neoadjuvant endocrine treatment is associated with favorable breast cancer relapse free and overall survival (17, 18). Although this single-arm study was designed based on the rates of CCCA observed in previous neoadjuvant aromatase inhibitor (AI) studies, the added effect of palbociclib over that of anastrozole was determined by analysis of tumor biopsies collected at C1D1 following 4 weeks of cycle 0 anastrozole monotherapy, and at C1D15, 2 weeks after the addition of palbociclib to anastrozole. CCCA and Ki67

responses were assessed by *PIK3CA* mutation status because of the alternative strategy of *PIK3CA*-targeted therapy in the mutation-positive population. Secondary objectives included analysis of CCCA and Ki67 response by baseline PAM50-based intrinsic subtypes, and assessment of clinical, radiological, and pathologic response and safety profiles. Exploratory biomarker studies included gene expression and somatic mutation profiling.

Patient Population and Methods

Eligibility

Eligible patients included pre- and postmenopausal women at least 18 years old, with a clinical stage II/III, ER⁺ (Allred score 6–8) and HER2⁻ (0 or 1+ by IHC or FISH negative) invasive breast cancer. Additional eligibility criteria included: Eastern Cooperative Oncology Group Performance Status of 0 to 2, adequate organ, and marrow function. For patients receiving goserelin, estradiol level in the postmenopausal range was required to receive further treatment on study. Exclusion criteria included prior treatment of the current cancer, uncontrolled intercurrent illness, active or recent coronary events, cerebrovascular accident, symptomatic pulmonary embolism or congestive heart failure, known HIV-positivity, metastatic disease, inflammatory cancer, previous excisional biopsy of the breast or sentinel lymph node, corrected QT > 470 msec, allergic reactions to compounds similar to palbociclib, pregnant/nursing, or taking anticoagulation, medications that prolong QT or are known CYP3A4 inhibitors. The study was approved by Institutional Review Board at participating sites and followed the Declaration of Helsinki and Good Clinical Practice guidelines. Written informed consent was required.

Study design and treatment

The primary endpoint was CCCA (Ki67 ≤ 2.7%) on palbociclib plus anastrozole at C1D15. The study was designed to ensure the sample size for the *PIK3CA* WT cohort and the overall population for the primary endpoint analysis. A sample size of 33 in the *PIK3CA* WT cohort was chosen based on the Fleming's single-stage phase II design to test the hypothesis that palbociclib plus anastrozole leads to at least 50% improvement over anastrozole alone in CCCA rates [44% with anastrozole based on historical data (19) vs. 66% with palbociclib plus anastrozole, power = 0.8, alpha = 0.05]. The primary endpoint is met if more than 20 of 33 patients achieved CCCA. Patients were prospectively assigned to *PIK3CA* WT or Mut Cohort at C1D1 based on CLIA *PIK3CA* sequencing. Based on the prevalence of *PIK3CA* mutation, we estimated that 14 to 17 patients would enroll to the exploratory *PIK3CA* Mut cohort with 33 patients to the *PIK3CA* WT cohort. If 10 of 15 achieved CCCA in the *PIK3CA* Mut cohort, the 80% confidence for the "true" rate would be 47% to 83%.

Eligible patients were preregistered, underwent baseline tumor biopsy (C0D1), and began cycle 0 anastrozole (1 mg PO daily for 4 weeks) and goserelin (3.6 mg subcutaneous each 28 days) if premenopausal, while *PIK3CA* sequencing was being performed. Palbociclib (125 mg PO daily on days 1–21 each 28-day cycle) was started on C1D1 after tumor biopsy (second biopsy time point) and registration to *PIK3CA* WT or Mut Cohort. Patients with unsuccessful *PIK3CA* sequencing due to DNA quality or quantity not sufficient (QNS) also received therapy per protocol. Tumor biopsy was again performed on

C1D15 (third biopsy time point) for CLIA Ki67 analysis. If C1D15 Ki67 > 10%, protocol therapy was discontinued due to inadequate response. Patients with C1D15 Ki67 ≤ 10% (or indeterminate) continued palbociclib and anastrozole for 4 cycles unless patients experienced intolerable side effects, disease progression, estradiol level in premenopausal range while receiving goserelin, or withdrew. Surgery occurred 3 to 5 weeks after the last dose of palbociclib to allow adverse event (AE) recovery. Following a protocol amendment, patients whose absolute neutrophil count (ANC) recovered to >1.5 k/mcL, platelet >100 k/mcL, and nonhematologic AEs to ≤grade 1 within 3 weeks after completion of cycle 4 received additional 10 to 12 days of cycle 5 palbociclib immediately before surgery. Anastrozole (with goserelin if premenopausal) was administered until surgery. Uniform biopsy/shipment kits were provided (18, 19).

Clinical tape/caliper bidimensional tumor measurement and AE assessment by CTCAE 4.0 were performed on day 1 of each cycle. Serum estradiol levels were tested on C1D1 and C3D1. Radiological assessment by mammogram and ultrasound was required at baseline and prior to surgery. Clinical tumor response was assessed by World Health Organization (WHO) criteria and radiologic response by RECIST 1.1.

CLIA PIK3CA sequencing

PIK3CA (ref seq# NM_006218) sequencing of exons 2, 5, 8, 10 and 21, and exon-intron splice junctions was performed on tumor DNA from the baseline biopsy at the CLIA-certified Washington University Genomic and Pathology Service initially by Sanger ($n = 18$), subsequently by next-generation sequencing (NGS; $n = 32$). The targeted exons were PCR amplified using the (Fluidigm Corp.) 48.48 high-throughput access array system. Cluster generation and sequencing were performed using the Illumina's HiSeq2500 Reagent Kit (200 cycles), and 2×101 paired-end sequence reads were generated. Each patient's tumor DNA was processed and sequenced in three independent technical replicates. The three fastq files were each aligned independently to the human reference genome hg19 NCBI build 37.2 to generate three BAM files, and then merged to a single BAM file. Sequence analysis was performed on all four BAM files using a combination of commercially available and custom-developed scripts to generate a multisample VCF file. Alignment to the human reference genome was performed using Novoalign 2.08.02, sorting and indexing were performed by SAMtools 0.1.18-1, with coverage calculation by BedTools 2.13.3 and variants calling by FreeBayes 0.9.7. Variants were called if present in at least three of the four BAM files and the average variant allele frequency (VAF) ≥ 10%.

Ki67 IHC and quantification

Ki67 staining was performed centrally at the CAP/CLIA-certified AMP lab at Washington University using the CONFIRM anti-Ki67 antibody (clone 30-9) and scored using pathologist-guided imaging analysis as previously described (18, 19).

Gene expression analysis, PAM50 intrinsic subtype, and proliferation score

Total RNA from fresh-frozen tumor biopsies at baseline and subsequent time points was extracted when at least 50% tumor cellularity was present (19). Microarray gene expression data were generated on an Agilent microarray platform and normalized

(19), followed by PAM50-based intrinsic subtype assignment and the 11-gene proliferation score determination (19, 20).

83-gene panel next-generation sequencing

Tumor DNA extracted from fresh-frozen biopsies and matched leukocyte germline DNA were subjected to targeted Illumina NGS of an 83-gene panel (21–23). Mutation waterfall plot was created with GenVisr (24).

Statistical analysis

The rates of CCCA (overall and by subgroups) were the percentage of patients with tumor Ki67 ≤ 2.7% at C1D1 and C1D15. The corresponding 90% confidence intervals (CI) were calculated as normal approximation or binomial exact CI as appropriate. The rates of CCCA between C1D1 and C1D15 were compared using the McNemar test. The clinical response rate was the percentage of evaluable patients who met the WHO criteria of complete or partial response prior to surgery with 90% CI. The radiological response rate (by RECIST 1.1) was similarly calculated.

Changes in Ki67 over time and the differences between subgroups (*PIK3CA* Mut vs. WT, LumA vs. LumB subtypes, etc.) were analyzed using generalized estimating equation (25, 26), followed by a step-down Bonferroni adjustment for multiple comparisons. As Ki67 followed a right-skewed distribution, a logarithm transformation was performed. (25, 26) The gene expression data were analyzed to identify differentially expressed genes across time points (by F-test) and between time points (by moderated two sample *t* test) accounting for multiple measures from the same patient using the Bioconductor package limma (linear models for microarray data, version 3.20.9), and FDR-adjusted *P* values were reported (27). Enriched gene ontology terms were subsequently performed using GStats (version 2.30.0; ref. 28). All statistical analyses were performed using SAS 9.2 (SAS Institutes) except gene expression analyses which were performed using R 3.1.1 (<http://cran.r-project.org>). All reported *P* values were two-sided unless otherwise noted. The microarray data have been submitted to Gene Expression Omnibus (GEO; series accession number GSE93204).

Results

Enrollment

Between April 2013 and April 2015, 50 patients (18 pre- and 32 postmenopausal), median age 57.5 (range, 34.1–79.6) years, with clinical stage II/III ER⁺/HER2⁻ breast cancer enrolled to the study, which included 16 in the *PIK3CA* Mut, 32 in the *PIK3CA* WT cohort, and 2 with unknown *PIK3CA* status. Table 1 detailed the patient and tumor characteristics. Five patients were without C1D15 Ki67 value due to withdrawal ($n = 2$), inability to biopsy ($n = 2$), and insufficient biopsy material ($n = 1$), leaving 45 (16 *PIK3CA* Mut, 28 *PIK3CA* WT, and 1 *PIK3CA* unknown) evaluable for the primary endpoint (Supplementary Fig. S1). Five patients went off study per protocol due to C1D15 Ki67 > 10% ($n = 4$) and elevated estradiol on goserelin at C3D1 (62 pg/mL; $n = 1$). Thirty-nine patients completed neoadjuvant therapy and underwent definitive breast and axillary surgery. Following the protocol amendment that added cycle 5 prior to surgery, 10 patients received cycle 5 palbociclib and all underwent surgery as scheduled. Among these 10 patients, 1 mistakenly stopped her palbociclib

Table 1. Patient and tumor characteristics

Characteristic	Entire cohort (n = 50)	PIK3CA Mut (n = 16)	PIK3CA WT (n = 32)
Median age (range), years	57.5 (34.1–79.6)	55.2 (34.1–79.3)	57.7 (34.8–79.6)
Race			
White	47 (94%)	16 (100%)	29 (91%)
Black	3 (6%)	0	3 (9%)
Menopausal status			
Premenopausal	18 (36%)	8 (50%)	11 (34%)
Postmenopausal	32 (64%)	8 (50%)	21 (66%)
PgR Allred Score			
Neg	3 (6%)	0	3 (9%)
Pos	47 (94%)	16 (100%)	29 (91%)
Tumor grade			
1	12 (24%)	4 (25%)	7 (22%)
2	31 (62%)	11 (69%)	19 (59%)
3	7 (14%)	1 (6%)	6 (19%)
Histology			
Ductal	33 (66%)	11 (69%)	21 (66%)
Lobular/mixed	15 (30%)	4 (25%)	10 (31%)
Other (papillary, mucinous)	2 (4%)	1 (6%)	1 (3%)
Clinical stage			
II/IIA	20 (40%)	6 (38%)	14 (44%)
IIB	16 (32%)	8 (50%)	7 (22%)
IIIA	12 (24%)	2 (12%)	9 (28%)
IIIB/C	2 (4%)	0	2 (6%)
PAM50 intrinsic subtype	N = 32	N = 9	N = 23
LumA	17 (53%)	5 (56%)	12 (52%)
LumB	12 (38%)	3 (33%)	9 (39%)
HER2-E	1 (3%)	0	1 (4%)
Basal-like	1 (3%)	0	1 (4%)
Normal	1 (3%)	1 (11%)	0

early (5 days prior to surgery) despite normal ANC 1 week on cycle 5 and 1 had a planned 1-week delay in her surgery from the final dose of palbociclib due to physician concern of potential cytopenia since this patient experienced grade 3 ANC in previous cycles that led to a dose delay in cycle 4. Seven additional patients would have been eligible for cycle 5 but did not proceed due to scheduling and logistics ($n = 6$) and ANC not recovering to normal within 3 weeks after cycle 4 ($n = 1$).

Safety

All patients were evaluable for AE. Treatment was well tolerated. Common grade (G)₂ and above AEs (>10% incidence) included transient neutropenia (G₃, 22%; G₄, 4%), leukopenia, and fatigue (Supplementary Table S1). Seven (14%) patients required one dose-level reduction due to G₃ neutropenia with dose delay ($n = 3$), G₄ neutropenia ($n = 1$), G₃ elevated transaminases ($n = 2$), and G₂ rash ($n = 1$). No G₄ or above non-hematologic AEs or neutropenic fevers were observed.

Clinical, radiologic, and pathologic responses

Forty-one patients received at least 3 cycles of palbociclib and anastrozole, including 39 who underwent surgery, 1 refused surgery, and 1 subsequently withdrew, and were assessed for clinical and radiologic responses (Supplementary Table S2). The response rates (90% CI) were 80% (68%–90%), 41% (25%–58%), and 52% (35%–68%), by exam, ultrasound, and mammogram. Pathologic stages were as follows: I ($n = 7$), II ($n = 22$), and III ($n = 10$) at mastectomy ($n = 20$) or lumpectomy ($n = 19$). No pathologic complete responses were observed.

CCCA and Ki67 response in the overall population and by PIK3CA status

The rates of CCCA with palbociclib plus anastrozole were significantly higher at C1D15 than that at C1D1 with anastrozole monotherapy for all evaluable patients (87% vs. 26%, $P < 0.001$), PIK3CA Mut (100% vs. 25%, $P < 0.001$), and PIK3CA WT (79% vs. 25%, $P < 0.001$) cohorts (Table 2). The CCCA rates at C1D15 exceeded the predefined cut-point for meeting the primary endpoint of at least 66% in the overall, PIK3CA WT, and Mut cohorts. Of the 31 patients resistant to anastrozole (non-CCCA at C1D1), 26 (84%) responded to palbociclib (CCCA at C1D15). When considered as a continuous variable, Ki67 levels were significantly reduced from baseline C0D1 to C1D1 following anastrozole monotherapy ($P < 0.01$) and from C1D1 to C1D15 after adding palbociclib ($P < 0.01$) for both PIK3CA WT and Mut cohorts (Fig. 1A–C). There was a greater variability in Ki67 response among the PIK3CA WT tumors, which included all 6 palbociclib-resistant tumors (non-CCCA at C1D15; Fig. 1C).

CCCA and Ki67 response by intrinsic subtype

Thirty-two patients had sufficient tumor RNA extracted from frozen baseline biopsies for microarray gene expression analysis. PAM50 intrinsic subtype determination identified 17 Luminal A (LumA), 12 Luminal B (LumB), 1 basal-like, 1 HER2-Enriched (HER2-E; but HER2 negative by clinical criteria), and 1 normal-like assignment (Table 1). Significantly higher rates of CCCA were achieved at C1D15 compared with C1D1 in LumA (100% vs. 40%, $P = 0.008$) and LumB (75% vs. 9%, $P = 0.02$) tumors (Table 2). Seventeen of 21 (81%; 9/9 LumA, 8/10 LumB, and 0/2 nonluminal) tumors resistant to anastrozole subsequently achieved CCCA at C1D15. The subtypes of the six tumors resistant to palbociclib (C1D15 Ki67 > 2.7%) included 3 LumB, both nonluminal (1 basal-like, 1 HER2-E), and 1 subtype unknown (Supplementary Fig. S2). When considering Ki67 as a continuous variable, LumB tumors had significantly higher levels of Ki67 compared with Lum A tumors at C0D1 ($P < 0.01$). In addition, Ki67 levels were significantly reduced from baseline (C0D1) to C1D1 by anastrozole monotherapy ($P < 0.01$), and from C1D1 to C1D15 by the addition of palbociclib ($P < 0.01$) in both LumA and LumB tumors (Fig. 1D–F), indicating the efficacy of anastrozole and palbociclib in both luminal subtypes. Interestingly, the degree of Ki67 suppression by anastrozole ($P = 0.69$) and by the addition of palbociclib ($P = 0.97$) were similar between LumA and LumB tumors.

Ki67 recovery at surgery after palbociclib withdrawal

The first 29 patients completed 4 cycles of anastrozole plus palbociclib and underwent surgery following a median washout period of 29 (range, 8–49) days from C4D21 palbociclib. Anastrozole was continued until surgery. Ki67 was significantly higher at surgery than C1D15 ($P < 0.01$, $n = 23$ paired samples), but not significantly different from C1D1 ($P = 0.077$, adjusted for multiple comparisons; Fig. 1G and H). To test whether the Ki67 recovery was due to palbociclib withdrawal, subsequent patients ($n = 8$) received additional 10 to 12 days of palbociclib immediately before surgery (cycle 5). There was no significant differences in Ki67 levels between surgery and C1D15 time points in these patients ($P = 0.68$, $n = 7$ paired samples; Fig. 1G and I). Six of the 7 cases remained in CCCA at surgery (Fig. 1I), indicating the

Table 2. Rate of CCCA at C1D1 and C1D15, overall and by key subgroups

Variable	Levels	CCCA at C1D1		CCCA at C1D15		P value	CCCA at C1D15 in anastrozole-resistant cases ^a	
		N/total	% (90% CI)	N/total	% (90% CI)		N/total	% (90% CI)
All evaluable patients		12/46	26% (16%–39%)	39/45	87% (75%–94%)	<0.001	26/31	84% (69%–93%)
<i>PIK3CA</i>	WT	7/28	25% (12%–42%)	22/28	79% (62%–90%)	<0.001	14/19	74% (52%–89%)
	Mutant	4/16	25% (9%–48%)	16/16	100% (83%–100%)	<0.001	12/12	100% (78%–100%)
	QNS	1/2	50% (NE)	1/1	100% (NE)	–	–	–
Baseline intrinsic subtype	LumA	6/15	40% (19%–64%)	16/16	100% (83%–100%)	0.008	9/9	100% (72%–100%)
	LumB	1/11	9% (0%–36%)	9/12	75% (47%–93%)	0.020	8/10	80% (49%–96%)
	Normal	1/1	100% (NE)	1/1	100% (NE)	–	–	–
	Nonluminal	0/2	0% (NE)	0/2	0% (NE)	–	0/2	0% (NE)
Menopausal status	Pre	6/18	33% (16%–55%)	15/17	88% (67%–98%)	0.003	9/11	82% (53%–97%)
	Post	6/28	21% (10%–38%)	24/28	86% (70%–95%)	<0.001	17/20	85% (66%–96%)
Histology	Ductal	3/30	10% (3%–24%)	25/30	83% (68%–93%)	<0.001	20/25	80% (62%–92%)
	Lobular/mixed	8/14	57% (33%–79%)	12/13	92% (68%–100%)	0.103	5/5	100% (55%–100%)
	Others	1/2	50% (NE)	2/2	100% (NE)	–	1/1	100% (NE)
Tumor grade	G ₁	4/11	36% (14%–65%)	10/11	91% (64%–100%)	0.025	5/6	83% (42%–100%)
	G ₂	7/28	25% (12%–42%)	24/27	89% (74%–97%)	<0.001	17/19	89% (70%–98%)
	G ₃	1/7	14% (0%–52%)	5/7	71% (34%–95%)	0.046	4/6	67% (27%–94%)
PgR	Positive	12/43	28% (17%–41%)	38/42	90% (80%–97%)	<0.001	25/28	89% (75%–97%)
	Negative	0/3	0% (NE)	1/3	33% (NE)	–	1/3	33% (NE)
<i>PTEN</i>	WT	9/31	29% (16%–45%)	27/31	87% (73%–95%)	<0.001	18/21	86% (67%–96%)
	Mutant	1/8	13% (0%–47%)	7/8	88% (53%–100%)	0.014	6/7	86% (48%–100%)
<i>TP53</i>	WT	8/30	27% (14%–43%)	28/30	93% (80%–99%)	<0.001	20/21	95% (79%–100%)
	Mutant	2/9	22% (4%–55%)	6/9	67% (34%–90%)	0.046	4/7	57% (23%–87%)
<i>RB1</i>	WT	10/36	28% (16%–43%)	32/36	89% (76%–96%)	<0.001	22/25	88% (72%–97%)
	Mutant	0/3	0% (NE)	2/3 ^b	67% (NE)	–	2/3 ^b	67% (NE)

Abbreviation: NE, not evaluable.

^aAnastrozole resistance was defined as Ki67 > 2.7% (non-CCCA) at C1D1.

^bTwo (PD203 and PD131) of the 3 *RB1* mutant tumors had low-frequency *RB1* mutations and were resistant to anastrozole (C1D1 Ki67 > 2.7%) but sensitive to palbociclib (Ki67 ≤ 2.7%). PD203 (Ki67: baseline 36%, C1D1 27%, C1D15 34%) had *RB1* p.532N with VAFs (depth of coverage) of 5.4% (92x) at baseline, which was not identified at subsequent time points (C1D1, C1D15, and surgery). PD131 (Ki67: baseline 2.7%, C1D1 22%, C1D15 1%) had *RB1* p.A562P (VAF 4.7%) and p.S576* (VAF 6.8%) at baseline (coverage, 400x). Sequencing data for subsequent time points were not available for PD131. PD106 was resistant to both anastrozole and palbociclib (Ki67: baseline 38%, C1D1 40%, C1D15 48%) and had *RB1* p.E323fs with VAF of 11% (baseline) and 25% (C1D15; ~30x).

need for continuous therapy with palbociclib to maintain the antiproliferative effect.

Ki67 response by clinical, pathologic, and mutation profiles

To identify potential clinical and molecular response markers for palbociclib, we examined the rates of CCCA at C1D1 and C1D15 by menopausal status, histology, tumor grade, PgR status, and mutations identified in the 83-gene panel NGS (Supplementary Table S3). Palbociclib benefit was observed across all subsets, including tumors that were grade 3, negative for PgR, or harboring mutations in *TP53* or *PTEN*, which are known endocrine-resistant mechanisms (Table 2). *RB1* mutation was identified in 3 breast cancers, all with co-occurring *PTEN* mutations, at baseline (Fig. 2), including the *RB1* E323fs (VAF 11% at baseline, 25% at C1D1) mutant HER2-E tumor that was resistant to both anastrozole and palbociclib, and two other tumors resistant to anastrozole alone (C1D1 Ki67 > 2.7%) but sensitive to palbociclib (C1D15 Ki67 ≤ 2.7%): one LumB tumor with *RB1* I532N (VAF 5.4% at baseline, undetectable at C1D1, C1D15, and surgery) and the other (subtype unknown) carrying concurrent *RB1* A562P (VAF 4.7%)/S576* (VAF 6.8%) at baseline (no mutation data for subsequent time points).

Figure 2 details the somatic mutations available for 41 patients with anastrozole-sensitive (C1D1 Ki67 ≤ 2.7%; *n* = 9), palbociclib-sensitive (C1D1 Ki67 > 2.7% but C1D15 Ki67 ≤ 2.7%; *n* = 24), or -resistant (C1D15 Ki67 > 2.7%, *n* = 5) tumors (C1D1/C1D15 Ki67 missing, *n* = 3). In addition to *PIK3CA*, mutations in *CDH1*, *PTEN*, *TP53*, *TBX3*, and *MAP3K1* were most common. Five of the 6 resistant tumors had sufficient material for sequencing.

The HER2-E tumor carried an *RB1* pE323fs as discussed above, whereas the basal-like tumor harbored a *TP53* p.S127F mutation. The 3 LumB-resistant tumors carried *TP53* T18fs (*n* = 1), none (*n* = 1), or mutations in multiple genes (*ATR*, *MAP3K1*, *GATA3*, *MLL*, *BRCA2*, *FOXA1*, *AKT1*, and *CDH1*; *n* = 1). Overall, palbociclib was effective across tumors harboring a wide spectrum of somatic mutations.

Response by PAM50 proliferation score

To confirm the added antiproliferative effect of palbociclib over anastrozole based on Ki67 IHC, we also calculated the PAM50 proliferation score using the previously described 11-gene signature (20, 29) based on microarray data from each time point. The proliferation score was significantly reduced from baseline to C1D1 (*P* < 0.0001), and from C1D1 to C1D15 (*P* < 0.0001; Supplementary Fig. S3) and correlated with Ki67 data at all time-points (Supplementary Fig. S3B–S3E). A heat-map of the 11 proliferation genes in different response categories is shown in Supplementary Fig. S4. Similar to Ki67, recovery in the proliferation score was also observed at surgery, which was inhibited by cycle 5 palbociclib. These data provided further validation of the antiproliferative effects of palbociclib.

Gene expression changes induced by anastrozole alone and in combination with palbociclib

Agilent microarray for gene expression was performed using total RNA obtained from serial fresh-frozen tumor biopsies. Data were generated for 29,284 probes and 118 samples (baseline, *n* = 32; C1D1, *n* = 33; C1D15, *n* = 29; surgery, *n* = 24) for 46 patients.

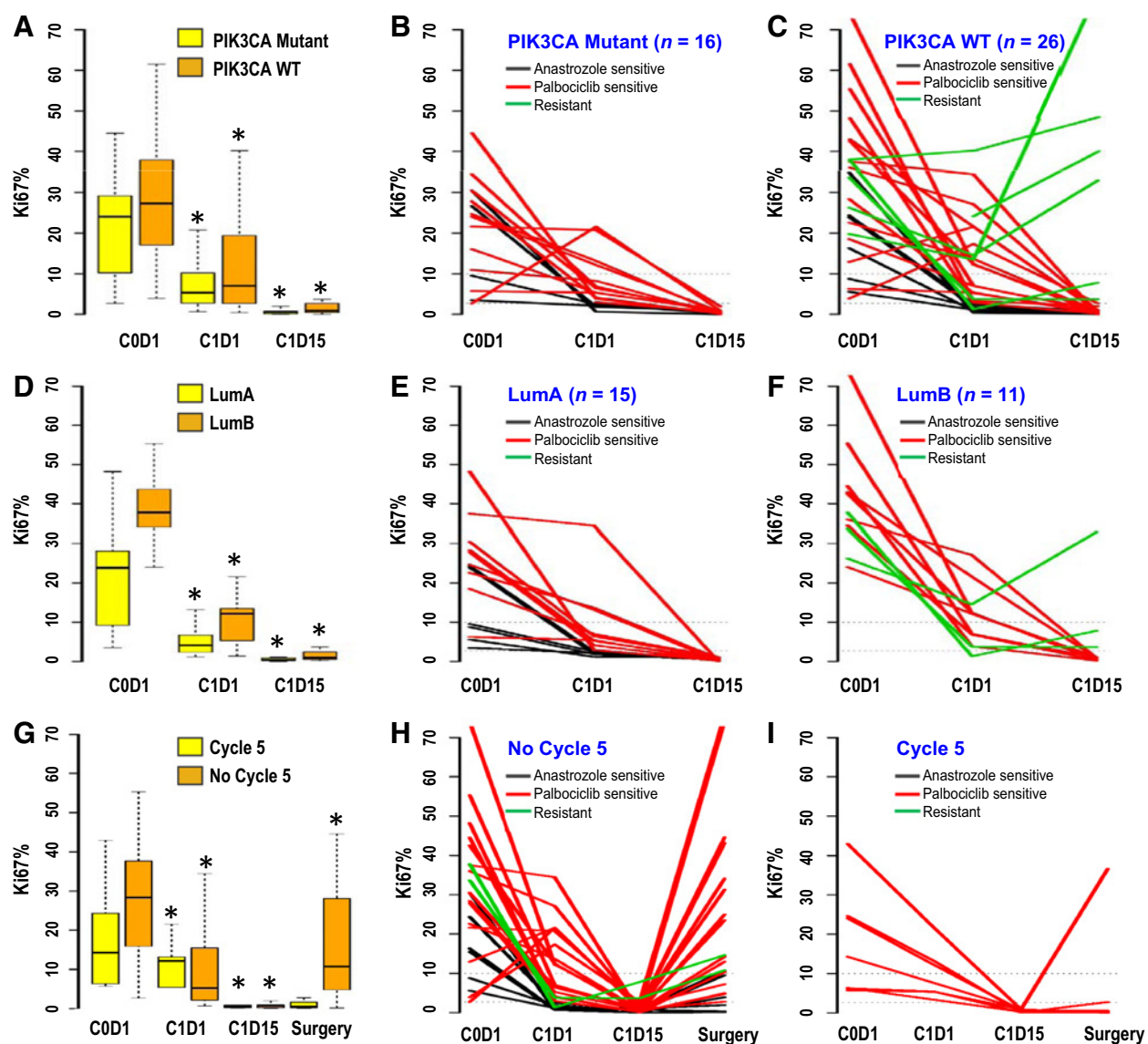


Figure 1.

Ki67 response by *PIK3CA* mutation status (A–C), luminal subtype (D–F), and with/without Cycle 5 (G–I). Box plots of all evaluable samples of indicated cohort (A, D, G) and Ki67 of individual tumors (B–C, E–F, H–I) are shown. *, $P < 0.005$ comparing Ki67 values with that of the previous time point in the corresponding cohort. Line colors in the Ki67 graphs denote response category (anastrozole sensitive, C1D1 Ki67 $\leq 2.7\%$; palbociclib sensitive, C1D1 Ki67 $> 2.7\%$ and C1D15 Ki67 $\leq 2.7\%$; resistant, C1D15 Ki67 $> 2.7\%$).

The expression levels of 1,538 genes (493 up and 1,045 down) were significantly altered by anastrozole (Fig. 3A). In contrast, only 6 genes, including *KIF15*, *CASC5*, *FAM64A*, *TOP2A*, *ASPM*, and *CEP55*, were significantly altered (downregulated) by adding palbociclib (C1D15 vs. C1D1), which were also among the genes downregulated by anastrozole and upregulated at surgery (Fig. 3B). A total of 235 (177 up and 58 down) genes were differentially expressed between surgery and C1D15. A number of classical ER-regulated genes were downregulated by anastrozole, including *PDZK1*, *MAPT*, *PgR*, *STC2*, *RABEP1*, *TTF3*, *CCND1*, *PREX1*, *HSPB8*, and *RABEP1*, which were not significantly altered by palbociclib (Supplementary Fig. S4 and Supplementary Table S4). The top biological pathways altered by anastrozole (C1D1 vs. C0D1) included mitotic cell cycle, nuclear division, mitosis,

and DNA replication, whereas the top pathways altered at the completion of neoadjuvant therapy (surgery vs. C1D15) also included programmed cell death and apoptotic process (Fig. 3C and Supplementary Table S4). Compared with C1D15, the surgical time point was associated with upregulation of genes that promote cell-cycle progression and a small set of genes that reduce apoptosis (Supplementary Table S4).

mRNA gene expression levels of G₁ cyclins, CDKs, and CDK inhibitors

We hypothesized that resistance to palbociclib was likely a result of deregulated G₁–S cell-cycle regulators. We therefore compared the mRNA expression levels of candidate genes, including *RB1*, *CCND1*, *CCND2*, *CCND3*, *CCNE1*, *CDK2*, *CDK4*, *CDK6*,

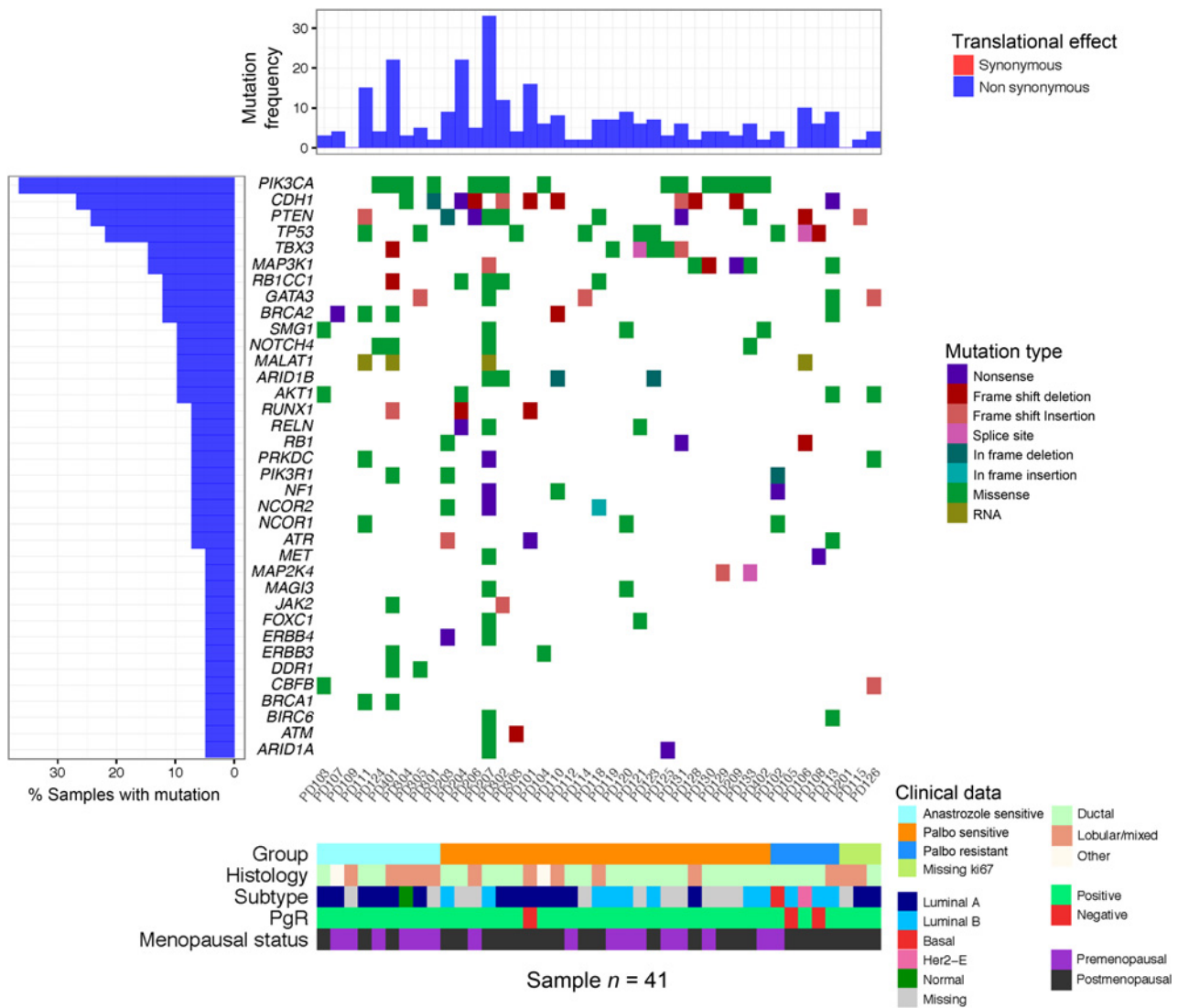


Figure 2. Somatic mutation, intrinsic subtype, and clinicopathologic characteristics of individual tumors in relation to Ki67 response. Genes with mutations detected in at least two samples are shown. Mutation frequency, number of tier 1 mutations.

CDKN2A, *CDKN2B*, *CDKN2C*, *CDKN2D*, *CDKN1A*, and *CDKN1B*, by response groups and time points. Pairwise two-sample *t* test analysis indicated significantly elevated expression of *CCND3*, *CCNE1*, and *CDKN2D* at C1D15 in the resistant group (Fig. 4). Interestingly, all three genes are transcriptionally regulated by E2F1 (30–32), suggesting persistent E2F activity in resistant tumors.

Discussion

The NeoPalAna trial demonstrated the potent antiproliferative effect of palbociclib in luminal breast cancers when the response to AI alone was incomplete. CCCA (Ki67 ≤ 2.7%) was achieved in 87% (90% CI, 75%–94%) at C1D15 (2 weeks after adding palbociclib), compared with the 28% (90% CI, 17%–41%) at C1D1 after 4 weeks of anastrozole monotherapy. The study met the primary endpoint in the overall population and

in both *PIK3CA* WT (79%; 90% CI, 62%–90%) and Mut cohorts (100%; 90% CI, 83%–100%; refs. 18, 19). Significant improvement in the rates of CCCA and inhibition of cell proliferation were observed in both LumA and LumB subtypes, and regardless of *PIK3CA* mutation, menopausal status, tumor histology, and grade. Palbociclib efficacy was observed across various genomic backgrounds that included somatic mutations in *PTEN*, *TP53*, and *RUNX1* which have been associated with endocrine resistance (33). Notably, the single HER2-E tumor which carried a *RB1* p.E323fs frameshift mutation was resistant to palbociclib as expected from preclinical studies (12). Two tumors sensitive to palbociclib by Ki67 (>2.7% at C1D1, ≤2.7% at C1D15) were found to have missense *RB1* mutations on baseline biopsies, PD131 (*RB1* p.A562P and p.S576*) and PD203 (*RB1* p.I532N—absent at subsequent time points). Although the sequencing depth was relatively high (92–400X), in the setting of low VAF, explanations for the disappearance

Downloaded from http://aacrjournals.org/clinccancerres/article-pdf/23/15/4055/2037430/4055.pdf by guest on 26 August 2022

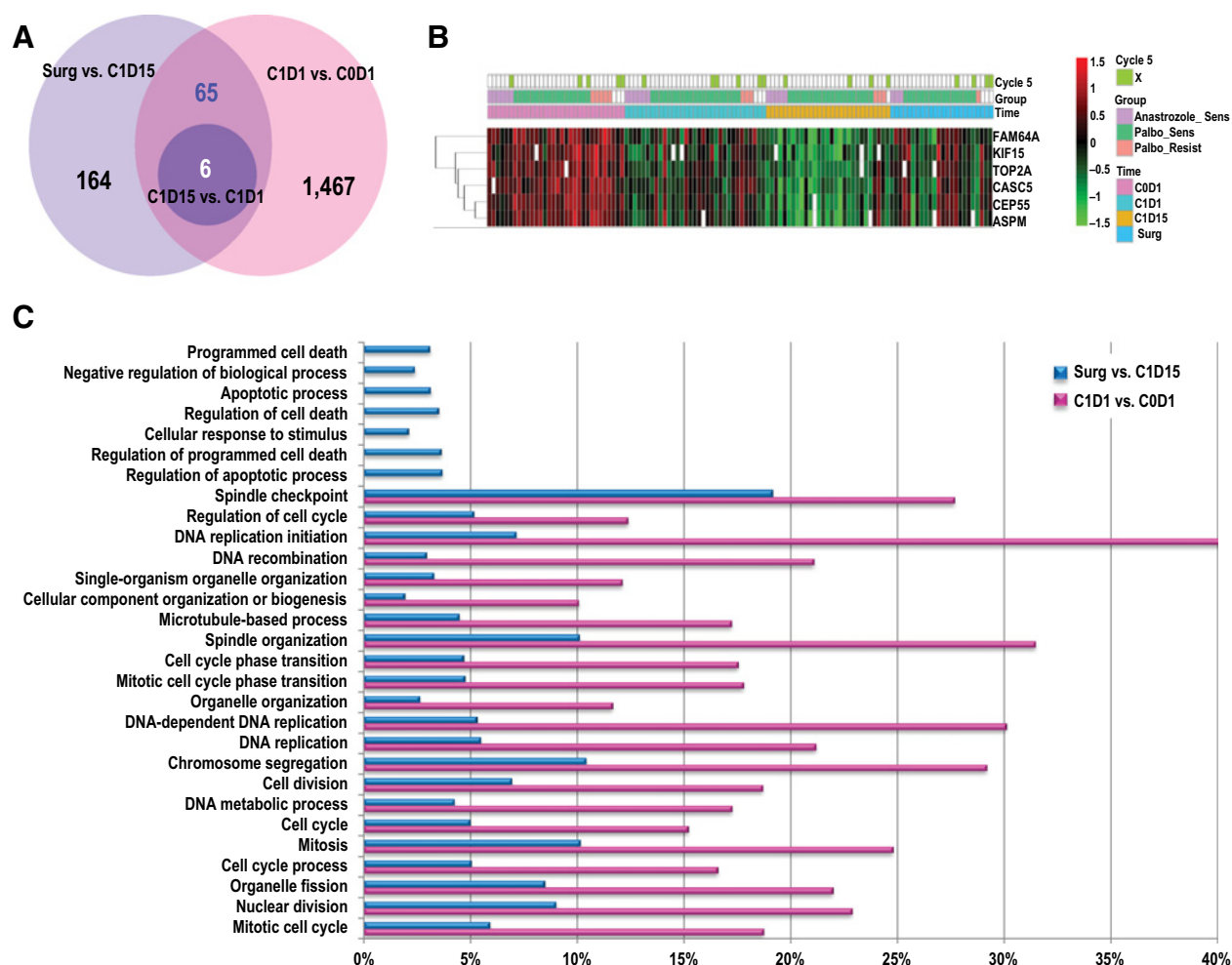


Figure 3. Microarray gene expression analysis. **A**, Venn diagram of the number of genes significantly changed (Benjamini–Hochberg FDR adjusted F test $P \leq 0.05$) between time points. **B**, Heatmap of the six genes significantly downregulated by anastrozole and by adding palbociclib. **C**, Top 20 significantly altered GO pathways comparing the gene expression profiles between C1D1 and COD1, or between surgery and C1D15. % indicates the percentage of genes observed in the indicated GO pathway.

of the *RB1* p.I532N at subsequent time points include intra-tumoral heterogeneity in potentially spatially separated biopsies (34), clonal evolution in response to treatment (22), or sequencing artifact.

The broad antitumor activity of palbociclib in luminal breast cancers observed in this trial is consistent with findings in preclinical studies (12) and in clinical trials of patients with advanced breast cancer (13–16). Although a previous presurgical window-of-opportunity study that randomized patients to receive 2 weeks of letrozole alone (Arm 1, $n = 2$), with ribociclib (Arm 2, 400 mg daily, $n = 6$), or ribociclib (Arm 3, 600 mg daily, $n = 3$) reported a mean decrease in Ki67 of 69% (38%–100%), 96% (78%–100%), and 92% (75%–100%), in Arms 1, 2, and 3, respectively, the small sample size limited the ability to conclude on the added antiproliferative effect of ribociclib to letrozole (35). The current study therefore provides the initial biomarker evidence of enhanced antiproliferative effect of a CDK4/6 inhibitor over that by an AI alone in primary breast cancers, supporting the investigation of

palbociclib in the adjuvant setting for both pre- and postmenopausal women with luminal breast cancer.

ER⁺ breast cancer is enriched for activating mutations in *PIK3CA* (36, 37), and there is significant interest in developing PI3K inhibitors based on promising preclinical data (38–40). However, the efficacy of pan-PI3K inhibitors in clinical trials has been limited by dose-limiting toxicities, including rash, diarrhea, and elevated transaminases (41), whereas alpha-specific inhibitors are still under clinical trial evaluation (NCT02340221 and NCT02437318). The potent antiproliferative effect and well-tolerated safety profile of palbociclib in both *PIK3CA* mutant and WT populations observed in this trial are consistent with data from PALOMA-3 in which the addition of palbociclib to fulvestrant significantly improved PFS regardless of *PIK3CA* mutation status in patients with metastatic breast cancer by cell-free tumor DNA analysis (42). Interestingly, all six resistant tumors in the current trial were *PIK3CA* WT. This apparent association, however, could be due to the fact that all *PIK3CA* mutant tumors analyzed were luminal, whereas 2 of the *PIK3CA* WT tumors were nonluminal.

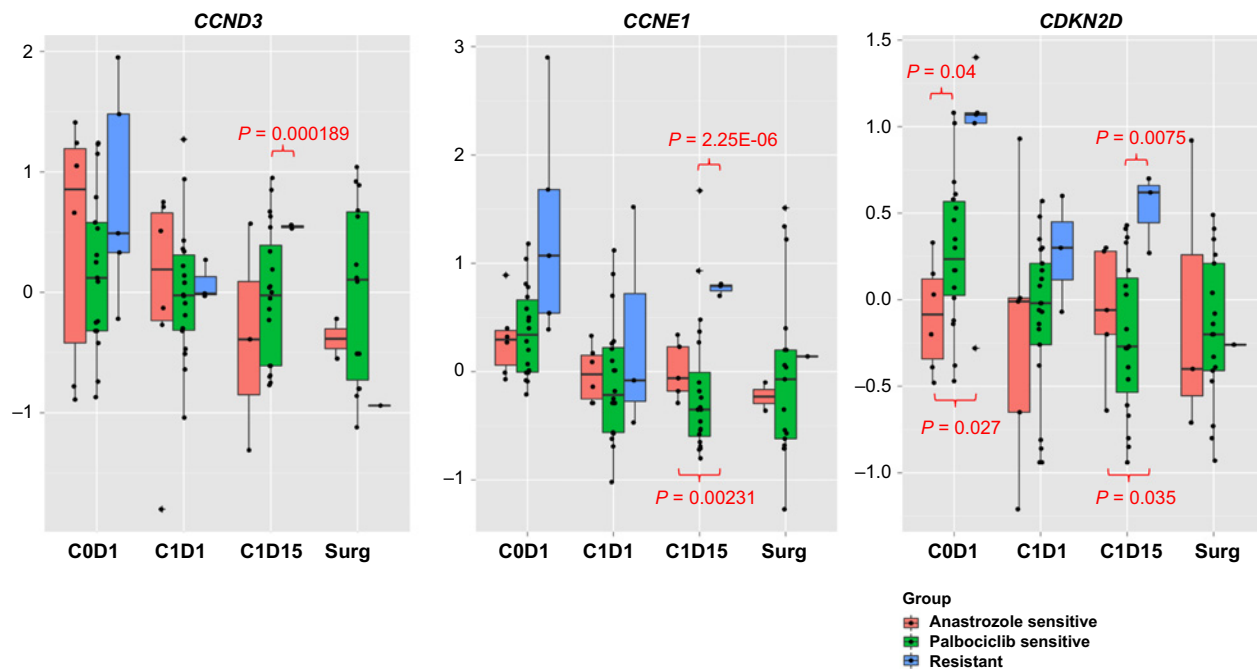


Figure 4.

Boxplots of gene expression levels of *CCND3*, *CCNE1*, and *CDKN2D* by Ki67 response and by time point. Significant *P* values by pairwise two-sample *t* test were indicated. The sample sizes for anastrozole-sensitive, palbociclib-sensitive, and resistant groups were 6, 18, and 5 at C0D1; 6, 21, and 3 at C1D1; 5, 20, and 3 at C1D15; and 3, 17, and 1 at surgery time points, respectively.

Because a large majority of *PIK3CA* WT tumors were responsive to palbociclib, the decision to use a CDK4/6 inhibitor should not be based on *PIK3CA* mutation status. However, it is possible that we might have enriched for a more resistant population in this trial due to the initial focus of enrollment to the *PIK3CA* WT cohort (43).

The rebound Ki67 at surgery was suppressed when palbociclib (cycle 5) was administered before surgery. This finding indicates that the antiproliferative effect of palbociclib is reversible despite 4 months of therapy. Nevertheless, the data indicate continued dosing beyond 4 months will be needed in the adjuvant setting. Interestingly, 1 patient showed elevated Ki67 at surgery despite the initial CCCA at C1D15 and cycle 5 palbociclib, suggesting the development of acquired resistance.

To avoid preanalytical, analytical, and scoring variations in Ki67 analysis, this trial employed a standardized sample acquisition method by providing biopsy/shipment kits, centralized processing, Ki67 staining, and pathologist-guided imaging analysis that have shown to yield reproducible Ki67 levels predictive of clinical outcomes (18). Importantly, the antiproliferation effect of palbociclib over that of anastrozole alone based on Ki67 was replicated by the PAM50 11-gene proliferation score and the gene expression pathway analysis in this study, providing the feasibility and validity of centralized CLIA Ki67 as a biomarker endpoint in multi-center neoadjuvant trials.

Despite the eligibility requirement for ER-rich tumors, the molecular characteristics of the tumor population were quite heterogeneous. The PAM50 analysis supports the use of palbociclib in both LumA and LumB breast cancers; however, the benefit of palbociclib may be particularly important for LumB tumors as they more often exhibit persistent tumor proliferation

on AI alone and carry a worse prognosis. Consistent with preclinical observations, neither the nonluminal breast cancers responded to palbociclib in this study (12). These data point to the potential value of PAM50 subtyping in clinical trials of CDK4/6 inhibitors.

The three response groups based on Ki67 levels at C1D1 and C1D15 clearly indicated that a subset of breast cancers (12/46, 26%) were able to achieve CCCA by anastrozole alone. However, no clear baseline biomarkers exist to date to identify this population for whom palbociclib could potentially be avoided (44, 45). The sequential treatment approach and on-treatment biomarker analysis illustrated by NeoPalAna could therefore offer a platform for individualized response assessment and treatment recommendations.

In addition to nonluminal subtype as a potential resistant marker for palbociclib, gene expression analysis of G₁ cyclins, CDKs, and CDK inhibitors indicated that resistance to palbociclib appeared to be associated with persistently elevated on-treatment expression of *CCND3*, *CCNE1*, and *CDKN2D*. Interestingly, all three genes are known E2F1 transcription targets which are expected to be downregulated upon CDK4/6 inhibition (30–32, 46). The association between *CCNE1* gain and resistance to CDK4/6 inhibition, likely through activation of CDK2, has been observed in preclinical studies (46). Our findings are hypothesis generating and warrant further investigations in larger sample sets.

Microarray analysis demonstrated that anastrozole significantly inhibited classical ER-regulated genes and cell-cycle pathways, findings consistent with previously reported neoadjuvant AI-induced gene expression changes (47–49). Although adding palbociclib further reduced cell proliferation, no significant

change in the expression of ER-regulated genes was observed between C1D1 and C1D15, consistent with the selective action of palbociclib on CDK4/6. Strikingly, only six genes were further significantly reduced in their levels of expression at C1D15 compared with C1D1, illustrating the tight association between ER signaling and CDK4/6 activation.

This study has several limitations, including the moderate sample size and the lack of long-term follow up data to correlate with Ki67 response. Although we clearly observed three response categories with respect to sensitivity to anastrozole alone and to the addition of palbociclib, the small sample size limited our ability to elucidate the underlying molecular mechanisms of palbociclib resistance. The findings of nonluminal subtype and persistent E2F target genes expression in palbociclib-resistant tumors require further validation in other studies.

In summary, this 50-patient single-arm, two-cohort (*PIK3CA* WT and *PIK3CA* Mut), multi-center neoadjuvant phase II study provided proof of principle regarding the ability of CDK4/6 inhibition to overcome intrinsic endocrine resistance in primary breast cancer across a wide range of somatic mutation profiles. The association of treatment resistance with nonluminal subtype and persistent on-treatment expression of E2F targets, including *CCND3*, *CCNE1*, and *CDKN2D*, indicates persistent activation of E2F transcription in resistant tumors and warrants further investigation of alternative cell-cycle inhibition approaches for this tumor subset.

Disclosure of Potential Conflicts of Interest

C.X. Ma is a consultant/advisory board member for Novartis and Pfizer Inc. M. Goetz is a consultant/advisory board member for Eli Lilly and Company. M. Naughton reports receiving speakers bureau honoraria from Pfizer Inc. M.J. Ellis is an employee of Bioclassifier, holds ownership interest (including patents) in Prosig/Nanostring, and is a consultant/advisory board member for Pfizer Inc. No potential conflicts of interest were disclosed by the other authors.

Authors' Contributions

Conception and design: C.X. Ma, J. Margenthaler, T.J. Eberlein, C.H. Bartlett, M. Koehler, M.J. Ellis

References

- Sherr CJ. Cancer cell cycles. *Science* 1996;274:1672–7.
- Sherr CJ, Roberts JM. CDK inhibitors: Positive and negative regulators of G1-phase progression. *Genes Dev* 1999;13:1501–12.
- van den Heuvel S, Harlow E. Distinct roles for cyclin-dependent kinases in cell cycle control. *Science* 1993;262:2050–4.
- Weinberg R. The retinoblastoma protein and cell cycle control. *Cell* 1995;81:323–30.
- Weintraub SJ, Prater CA, Dean DC. Retinoblastoma protein switches the E2F site from positive to negative element. *Nature* 1992;358:259–61.
- Altucci L, Addeo R, Cicatiello L, Germano D, Pacilio C, Battista T, et al. Estrogen induces early and timed activation of cyclin-dependent kinases 4, 5, and 6 and increases cyclin messenger ribonucleic acid expression in rat uterus. *Endocrinology* 1997;138:978–84.
- Geum D, Sun W, Paik SK, Lee CC, Kim K. Estrogen-induced cyclin D1 and D3 gene expressions during mouse uterine cell proliferation in vivo: Differential induction mechanism of cyclin D1 and D3. *Mol Reprod Dev* 1997;46:450–8.
- Said TK, Conneely OM, Medina D, O'Malley BW, Lydon JP. Progesterone, in addition to estrogen, induces cyclin D1 expression in the murine mammary epithelial cell, in vivo. *Endocrinology* 1997;138:3933–9.
- Tong W, Pollard JW. Progesterone inhibits estrogen-induced cyclin D1 and cdk4 nuclear translocation, cyclin E- and cyclin A-cdk2 kinase activation, and cell proliferation in uterine epithelial cells in mice. *Mol Cell Biol* 1999;19:2251–64.

Development of methodology: C.X. Ma, T.J. Eberlein, O.L. Griffith, C.H. Bartlett, H. Al-Kateb, M.J. Ellis

Acquisition of data (provided animals, acquired and managed patients, provided facilities, etc.): C.X. Ma, D.W. Northfelt, M. Goetz, A. Forero, J. Hoog, M. Naughton, F. Ademuyiwa, R. Suresh, K.S. Anderson, J. Margenthaler, R. Aft, T. Hobday, T. Moynihan, W. Gillanders, A. Cyr, T.J. Eberlein, T. Hieken, H. Krontiras, M.V. Lee, C. Bumb, S. Sanati, M.J. Ellis

Analysis and interpretation of data (e.g., statistical analysis, biostatistics, computational analysis): C.X. Ma, F. Gao, J. Luo, D.W. Northfelt, A. Forero, M. Naughton, T.J. Eberlein, T. Hieken, N.C. Spies, Z.L. Skidmore, O.L. Griffith, M. Griffith, S. Thomas, K. Vij, C.H. Bartlett, M. Koehler, H. Al-Kateb, M.J. Ellis

Writing, review, and/or revision of the manuscript: C.X. Ma, F. Gao, J. Luo, D.W. Northfelt, M. Goetz, A. Forero, M. Naughton, F. Ademuyiwa, K.S. Anderson, J. Margenthaler, T. Hobday, T. Moynihan, W. Gillanders, A. Cyr, T.J. Eberlein, T. Hieken, Z. Guo, Z.L. Skidmore, O.L. Griffith, M. Griffith, K. Vij, C.H. Bartlett, M. Koehler, H. Al-Kateb, M.J. Ellis

Administrative, technical, or material support (i.e., reporting or organizing data, constructing databases): C.X. Ma, J. Hoog, S. Thomas, M.J. Ellis

Study supervision: C.X. Ma, D.W. Northfelt, M. Goetz, A. Forero, T.J. Eberlein, O.L. Griffith, M.J. Ellis

Acknowledgments

The authors thank the patients and families who participated in this study and the staff who cared for these patients. We thank Stephanie Myles for assistance in protocol development, the Siteman Cancer Center Tissue Procurement Core, McDonnell Genome Institute, Genomic and Pathology Service, and Anatomical and Molecular Pathology Laboratory.

Grant Support

This work is funded in part by Siteman Cancer Center Grant (P30 CA91842, SCC, T.J. Eberlein), NCI Cancer Clinical Investigator Team Leadership Award (3P30 CA091842-12S2, NIH/NCI, C.X. Ma), Susan G. Komen Promise Grant (M.J. Ellis), Saint Louis Men's Group Against Cancer (C.X. Ma), and Pfizer Pharmaceuticals. Dr. O.L. Griffith is supported by the National Cancer Institute (NIH NC1K22CA188163). Dr. M.J. Ellis is a McNair Medical Institute Scholar and a Cancer Prevention Institute of Texas Senior Investigator.

The costs of publication of this article were defrayed in part by the payment of page charges. This article must therefore be hereby marked *advertisement* in accordance with 18 U.S.C. Section 1734 solely to indicate this fact.

Received December 20, 2016; revised December 19, 2016; accepted March 1, 2017; published OnlineFirst March 7, 2017.

- Thangavel C, Dean JL, Ertel A, Knudsen KE, Aldaz CM, Witkiewicz AK, et al. Therapeutically activating RB: Reestablishing cell cycle control in endocrine therapy-resistant breast cancer. *Endocr Relat Cancer* 2011;18:333–45.
- Fry DW, Harvey PJ, Keller PR, Elliott WL, Meade M, Trchet E, et al. Specific inhibition of cyclin-dependent kinase 4/6 by PD 0332991 and associated antitumor activity in human tumor xenografts. *Mol Cancer Ther* 2004;3:1427–38.
- Finn RS, Dering J, Conklin D, Kalous O, Cohen DJ, Desai AJ, et al. PD 0332991, a selective cyclin D kinase 4/6 inhibitor, preferentially inhibits proliferation of luminal estrogen receptor-positive human breast cancer cell lines in vitro. *Breast Cancer Res* 2009;11:R77.
- Finn RS, Martin M, Rugo HS, Jones S, Im SA, Gelmon K, et al. Palbociclib and letrozole in advanced breast cancer. *N Engl J Med* 2016;375:1925–36.
- Finn RS, Crown JP, Ettl J, Schmidt M, Bondarenko IM, Lang I, et al. Efficacy and safety of palbociclib in combination with letrozole as first-line treatment of ER-positive, HER2-negative, advanced breast cancer: Expanded analyses of subgroups from the randomized pivotal trial PALOMA-1/TRIO-18. *Breast Cancer Res* 2016;18:67.
- Turner NC, Ro J, Andre F, Loi S, Verma S, Iwata H, et al. Palbociclib in hormone-receptor-positive advanced breast cancer. *N Engl J Med* 2015;373:209–19.
- Finn RS, Crown JP, Lang I, Boer K, Bondarenko IM, Kulyk SO, et al. The cyclin-dependent kinase 4/6 inhibitor palbociclib in combination with letrozole versus letrozole alone as first-line treatment of oestrogen receptor-

- positive, HER2-negative, advanced breast cancer (PALOMA-1/TRIO-18): A randomised phase 2 study. *Lancet Oncol* 2015;16:25–35.
17. Ellis MJ, Tao Y, Luo J, A'Hern R, Evans DB, Bhatnagar AS, et al. Outcome prediction for estrogen receptor-positive breast cancer based on postneoadjuvant endocrine therapy tumor characteristics. *J Natl Cancer Inst* 2008;100:1380–8.
 18. Ellis MJ, Suman VJ, Hoog J, Goncalves R, Sanati S, Creighton CJ, et al. Ki67 proliferation index as a tool for chemotherapy decisions during and after neoadjuvant aromatase inhibitor treatment of breast cancer: Results from the American College of Surgeons Oncology Group Z1031 Trial (Alliance). *J Clin Oncol* 2017;JCO2016694406.
 19. Ellis MJ, Suman VJ, Hoog J, Lin L, Snider J, Prat A, et al. Randomized phase II neoadjuvant comparison between letrozole, anastrozole, and exemestane for postmenopausal women with estrogen receptor-rich stage 2 to 3 breast cancer: Clinical and biomarker outcomes and predictive value of the baseline PAM50-based intrinsic subtype-ACOSOG Z1031. *J Clin Oncol* 2011;29:2342–9.
 20. Nielsen TO, Parker JS, Leung S, Voduc D, Ebbert M, Vickery T, et al. A comparison of PAM50 intrinsic subtyping with immunohistochemistry and clinical prognostic factors in tamoxifen-treated estrogen receptor-positive breast cancer. *Clin Cancer Res* 2010;16:5222–32.
 21. Ma CX, Luo J, Naughton M, Ademuyiwa F, Suresh R, Griffith M, et al. A phase I trial of BKM120 (Buparlisib) in combination with fulvestrant in postmenopausal women with estrogen receptor-positive metastatic breast cancer. *Clin Cancer Res* 2016;22:1583–91.
 22. Miller CA, Gindin Y, Lu C, Griffith OL, Griffith M, Shen D, et al. Aromatase inhibition remodels the clonal architecture of estrogen-receptor-positive breast cancers. *Nat Commun* 2016;7:12498.
 23. Griffith M, Griffith OL, Smith SM, Ramu A, Callaway MB, Brummett AM, et al. Genome modeling system: A knowledge management platform for genomics. *PLoS Comput Biol* 2015;11:e1004274.
 24. Skidmore ZL, Wagner AH, Lesurf R, Campbell KM, Kunisaki J, Griffith OL, et al. GenVisR: Genomic visualizations in R. *Bioinformatics* 2016;32:3012–4.
 25. Liang K-Y, Zeger SL. Longitudinal data analysis using generalized linear models. *Biometrika* 1986;73:13–22.
 26. Hochberg Y, Tamhane AC. Multiple comparison procedures. New York: John Wiley & Sons, Inc.; 2008.
 27. Ritchie ME, Phipson B, Wu D, Hu Y, Law CW, Shi W, et al. Limma powers differential expression analyses for RNA-sequencing and microarray studies. *Nucleic Acids Res* 2015;43:e47.
 28. Falcon S, Gentleman R. Using GOstats to test gene lists for GO term association. *Bioinformatics* 2007;23:257–8.
 29. Prat A, Parker JS, Karginova O, Fan C, Livasy C, Herschkowitz JJ, et al. Phenotypic and molecular characterization of the claudin-low intrinsic subtype of breast cancer. *Breast Cancer Res* 2010;12:R68.
 30. Ma Y, Yuan J, Huang M, Jove R, Cress WD. Regulation of the cyclin D3 promoter by E2F1. *J Biol Chem* 2003;278:16770–6.
 31. Geng Y, Eaton EN, Picon M, Roberts JM, Lundberg AS, Gifford A, et al. Regulation of cyclin E transcription by E2Fs and retinoblastoma protein. *Oncogene* 1996;12:1173–80.
 32. Carcagno AL, Marazita MC, Ogara MF, Ceruti JM, Sonzogni SV, Scassa ME, et al. E2F1-mediated upregulation of p19INK4d determines its periodic expression during cell cycle and regulates cellular proliferation. *PLoS One* 2011;6:e21938.
 33. Ellis MJ, Ding L, Shen D, Luo J, Suman VJ, Wallis JW, et al. Whole-genome analysis informs breast cancer response to aromatase inhibition. *Nature* 2012;486:353–60.
 34. Gellert P, Segal CV, Gao Q, Lopez-Knowles E, Martin LA, Dodson A, et al. Impact of mutational profiles on response of primary oestrogen receptor-positive breast cancers to oestrogen deprivation. *Nat Commun* 2016;7:13294.
 35. Curigliano G, Gómez Pardo P, Meric-Bernstam F, Conte P, Lolkema MP, Beck JT, et al. Ribociclib plus letrozole in early breast cancer: A presurgical, window-of-opportunity study. *The Breast* 2016;28:191–8.
 36. Saal LH, Holm K, Maurer M, Memeo L, Su T, Wang X, et al. PIK3CA mutations correlate with hormone receptors, node metastasis, and ERBB2, and are mutually exclusive with PTEN loss in human breast carcinoma. *Cancer Res* 2005;65:2554–9.
 37. Network TCGA. Comprehensive molecular portraits of human breast tumours. *Nature* 2012;490:61–70.
 38. Crowder RJ, Phommaly C, Tao Y, Hoog J, Luo J, Perou CM, et al. PIK3CA and PIK3CB inhibition produce synthetic lethality when combined with estrogen deprivation in estrogen receptor-positive breast cancer. *Cancer Res* 2009;69:3955–62.
 39. Miller TW, Balko JM, Fox EM, Ghazoui Z, Dumbier A, Anderson H, et al. ERalpha-dependent E2F transcription can mediate resistance to estrogen deprivation in human breast cancer. *Cancer Discov* 2011;1:338–51.
 40. Ma CX, Crowder RJ, Ellis MJ. Importance of PI3-kinase pathway in response/resistance to aromatase inhibitors. *Steroids* 2011;76:750–2.
 41. Krop IE, Mayer IA, Ganju V, Dickler M, Johnston S, Morales S, et al. Pictilisib for oestrogen receptor-positive, aromatase inhibitor-resistant, advanced or metastatic breast cancer (FERGI): A randomised, double-blind, placebo-controlled, phase 2 trial. *Lancet Oncol* 2016;17:811–21.
 42. Cristofanilli M, Turner NC, Bondarenko I, Ro J, Im SA, Masuda N, et al. Fulvestrant plus palbociclib versus fulvestrant plus placebo for treatment of hormone-receptor-positive, HER2-negative metastatic breast cancer that progressed on previous endocrine therapy (PALOMA-3): Final analysis of the multicentre, double-blind, phase 3 randomised controlled trial. *Lancet Oncol* 2016;17:425–39.
 43. Vora SR, Juric D, Kim N, Mino-Kenudson M, Huynh T, Costa C, et al. CDK 4/6 inhibitors sensitize PIK3CA mutant breast cancer to PI3K inhibitors. *Cancer Cell* 2014;26:136–49.
 44. Ma CX, Reinert T, Chmielewska I, Ellis MJ. Mechanisms of aromatase inhibitor resistance. *Nat Rev Cancer* 2015;15:261–75.
 45. Ma CX, Bose R, Ellis MJ. Prognostic and predictive biomarkers of endocrine responsiveness for estrogen receptor positive breast cancer. *Adv Exp Med Biol* 2016;882:125–54.
 46. Herrera-Abreu MT, Palafox M, Asghar U, Rivas MA, Cutts RJ, Garcia-Murillas I, et al. Early adaptation and acquired resistance to CDK4/6 inhibition in estrogen receptor-positive breast cancer. *Cancer Res* 2016;76:2301–13.
 47. Miller WR, Larionov A, Anderson TJ, Evans DB, Dixon JM. Sequential changes in gene expression profiles in breast cancers during treatment with the aromatase inhibitor, letrozole. *Pharmacogenomics J* 2012;12:10–21.
 48. Miller WR, Larionov AA, Renshaw L, Anderson TJ, White S, Murray J, et al. Changes in breast cancer transcriptional profiles after treatment with the aromatase inhibitor, letrozole. *Pharmacogenet Genomics* 2007;17:813–26.
 49. Mackay A, Urruticoechea A, Dixon JM, Dexter T, Fenwick K, Ashworth A, et al. Molecular response to aromatase inhibitor treatment in primary breast cancer. *Breast Cancer Res* 2007;9:R37.